

Original paper

## Actions of mesenchymal stem cell secretome on microglia amyloid- $\beta$ uptake

Yoshikazu Yonei<sup>1)</sup>, Kyle Haasbroek<sup>1)</sup>, Shino Otaka<sup>2)</sup>, Chieko Sakiyama<sup>1)</sup>,  
Shohei Iwase<sup>3)</sup>, Masayuki Yagi<sup>1)</sup>

- 1) Anti-Aging Medical Research Center/Glycative Stress Research Center,  
Graduate School of Life and Medical Sciences, Doshisha University, Kyoto, Japan  
2) Sapporo Division, Cosmo Bio Co., Ltd., Otaru, Hokkaido, Japan  
3) Drug Discovery and Contract Services Division, Cosmo Bio Co., Ltd., Tokyo, Japan

### Abstract

In the brains of elderly dementia patients, important proteins (*i.e.*, amyloid  $\beta$  [A $\beta$ ], tau, and  $\alpha$ -synuclein) undergo post-translational modification, polymerization, aggregation, and deposition in tissues. Glycative stress, a non-physiological factor inducing these phenomena, is a state of excess aldehydes, and is induced by hyperglycemia, a high-fat diet, and alcohol consumption. In the lipid-rich brain, concurrently with carbohydrate-derived aldehydes, FA-derived aldehydes generated by the oxidation of FAs modify brain proteins like a double punch. Our previous reports have shown that glycated A $\beta$  can become resistant to microglia phagocytosis and may interfere with clearance. In this study, we created an A $\beta$  phagocytosis evaluation model using microglia-derived BV2 cells and evaluated the effects of mesenchymal stem cell secretome (SCST). SCST contains various growth factors and extracellular vesicles (EVs), and it has been reported that nasal administration improves symptoms in elderly dementia patients. Present results showed that SCST promotes A $\beta$  phagocytosis in a dose-dependent manner. These findings suggest that SCST may activate microglia and contribute to the homeostasis of A $\beta$  clearance. We speculate that it may also be important from the perspective of gliaprotection.

**KEY WORDS:** microglia, amyloid  $\beta$ , phagocytosis, dementia, stem cell secretome, gliaprotection

### Introduction

Various important proteins (*i.e.*, amyloid  $\beta$ , tau, and  $\alpha$ -synuclein) in the brains of elderly dementia patients undergo post-translational modification, polymerization, aggregation, and tissue deposition. Although the physiological role of amyloid beta (A $\beta$ ) is unknown, it plays an important role in the pathogenesis and progression of Alzheimer's disease (AD). It is said that A $\beta$  polymerization increases neurotoxicity, is difficult to decompose, and deposits in the brain, reducing A $\beta$  clearance. We focus on glycative stress (GS) as a risk factor for AD progression. GS is a state of aldehyde excess, caused by hyperglycemia, a high-fat diet, and excessive alcohol intake. In the lipid-rich brain, concurrently with carbohydrate-derived aldehydes, fatty acid (FA)-derived aldehydes generated by the oxidation of FAs induce a double punch of glycative modification of brain proteins.

In patients with diabetes, a typical disease with severe GS, various types of aldehydes including methylglyoxal (MGO) and acrolein (Acro) increase. Our previous studies have focused on A $\beta$  phagocytosis by microglia, which is involved in A $\beta$  clearance, and have examined the effects of GS. Glycated A $\beta$  is generated by MGO or Acro treatment. Fluorescence-labeled A $\beta$  (TAMRA-A $\beta$ ) and primary cultured mouse-derived microglia cells (Cosmo Bio Co., Ltd., Tokyo, Japan) were used in the experiments. Experiments using these cells have shown that microglia phagocytose A $\beta$ , while in contrast phagocytosis of glycated A $\beta$  is markedly reduced<sup>1)</sup>. When A $\beta$  was added to primary cultured microglia cells, there was a tendency for activation, proliferation, and natural death to decrease compared to when A $\beta$  was not added, so the possibility of neurotrophic gliaprotection should be seriously considered. Similar comments have been made in

Correspondence to: Professor Yoshikazu Yonei, MD, PhD  
Anti-Aging Medical Research Center,  
Graduate School of Life and Medical Sciences, Doshisha University  
1-3, Tatara Miyakodani, Kyotanabe, Kyoto, 610-0394 Japan  
TEL&FAX: +81-774-65-6394 e-mail: yyonei@mail.doshisha.ac.jp  
Co-authors; Haasbroek K, kylehaasbroek@gmail.com;  
Otaka S, shino-otaka@cosmobio.co.jp; Sakiyama C, csakiyam@mail.doshisha.ac.jp;  
Iwase S, shohei-iwase@cosmobio.co.jp; Sekiguchi S, shizuko-sekiguchi@cosmobio.co.jp;  
Yagi M. myagi@mail.doshisha.ac.jp

other papers<sup>2</sup>). In light of the above, it is considered important in preventive medicine to "improve A $\beta$  clearance and prevent the progression of AD" by lifestyle habits such as preventing glycation modification of A $\beta$  through GS care and improving "quality of sleep" rather than completely eliminating A $\beta$ .

Given this background, our laboratory, as stated in the Grant-in-Aid for Scientific Research application, began searching for components that promote or inhibit microglia A $\beta$  phagocytosis<sup>3</sup>. As a candidate substance, we are focusing on extracellular vesicles (EVs) derived from mutualistic bacteria in the gut microbiota.

During this period, Morita et al. reported that nasal administration of mesenchymal stem cell-derived secretome (SCST) improves the Hasegawa's dementia score in elderly patients with dementia<sup>4</sup>. There have been other similar reports<sup>5-7</sup>. We hypothesized that one of the mechanisms underlying the improvement of dementia symptoms is that SCST promotes microglia A $\beta$  phagocytosis. To verify this hypothesis, we examined the effect of SCST on phagocytosis in patients with dementia in an A $\beta$  phagocytosis model using BV2. If glial cells promote A $\beta$  phagocytosis, A $\beta$  clearance may improve. We hope that if factors that improve A $\beta$  clearance can be used, we will be able to obtain a useful means for preventing the progression and exacerbation of AD.

## Methods

### *From primary cultured microglia cells to cell lines*

The established cell lines used in microglia experiments to date have retained macrophage-like properties, and are said to differ significantly from *in vivo* microglia in terms of their response to inflammation and neuroprotection. Primary cultured microglia are prepared from the brain immediately after birth, and are grown in a mixed culture system that mainly contains astrocytes and neurons in addition to microglia, thereby maintaining the original functions of microglia<sup>8</sup>. In previous studies, a rat primary microglia culture kit (Cosmo Bio) was used to verify the function of microglia, which is to recognize and eliminate A $\beta$ <sup>9</sup>. Primary cultured cells are not suitable for an experimental model in which the efficacy of a relatively large number of samples is repeatedly evaluated due to large lot-to-lot differences. Therefore, the mouse microglia cell line BV2 (Code No.: 305156-Academic, Cell Lines Service GmbH, Germany) was used in this study.

### *Microglia cell line BV2*

BV2 cells are a type of microglia cell line derived from C57BL/6 mice that is widely used in animal experiments<sup>10,11</sup>. The cells were immortalized and established using a J2 retrovirus carrying the v-raf and v-myc oncogenes. BV2 cells express env gp70 antigen on their surface, which is one of the important features of BV2 cells, along with expression of nuclear v-myc and cytoplasmic v-RAF oncogenes. The env gp70 antigen contributes to the cell function in immune responses and inflammation in the brain.

BV2 cells were cultured in RPMI 1640 Medium (Thermo Fisher Scientific Inc.) supplemented with 10% fetal bovine serum (FBS) and Penicillin-Streptomycin (Fujifilm Wako Pure Chemicals) at 100 IU/mL, 0.1 mg/mL. For fluorescence

observation, phenol red-free medium was RPMI 1640 medium, no phenol red (Thermo Fisher Scientific Inc.) supplemented with 10% of FBS, penicillin-streptomycin (Fujifilm Wako Pure Chemicals) at 100 IU/mL, 0.1 mg/mL.

### *Synthesis of fluorescence-labeled A $\beta$ (TAMRA-A $\beta$ )*

The TAMRA-A $\beta$  used in the previous report<sup>1</sup> was fluorescently labeled TAMRA-A $\beta$  (Cosmo Bio). This reagent consists of A $\beta$ -(1-42) labeled with red fluorescent carboxytetramethylrhodamine (TAMRA) via a PEG spacer<sup>2</sup>.

The A $\beta$ -(1-42) peptide is a difficult reagent to handle. Its amphipathic sequence and strong self-aggregation tendency complicate characterization of both structure and function. Large lot-to-lot variations affect both aggregation behavior and biological activity. Dahlgren KN et al. recently took steps to minimize this variation by removing what they call "structural history"<sup>2</sup>. Structural history refers to secondary, tertiary, or quaternary structures that can act as templates or seeds and direct a large fraction of a peptide solution into a specific aggregation pathway. These structural seeds are not detected in synthetic products using traditional quality control methods that focus primarily on chemical purity and not on structural heterogeneity.

However, this A $\beta$ -(1-42) peptide, which has the property of good stability, was discontinued in 2022, and the stock was depleted. After that, we tried to use various commercially available fluorescence-labeled A $\beta$ , but we were unable to obtain labeled A $\beta$  suitable for the experiment due to unstable properties, poor solubility, and poor compatibility with primary microglia. Therefore, we decided to synthesize new A $\beta$ . The TAMRA-labeled mouse A $\beta$  used in this experiment was synthesized by the Sapporo Division of Cosmo Bio. The sequence was 5-TAMRA-XDAEFGHDSGFVRRHQKL VFFAEDVGSNKGAIIGLMVGGVVIA X:AEEAc (PEG), molecular weight 4975.57.

### *Verification of A $\beta$ phagocytosis*

#### **A $\beta$ pretreatment**

After dissolving mouse A $\beta$  in trifluoroacetic acid (TFA) (Nacalai Tesque) to 1 mg/mL, 100  $\mu$ L/tube of the dissolved solution was divided into two microtubes, diluted 10-fold with distilled water, and dried in a centrifuge evaporator. To loosen the aggregation of A $\beta$ , 100  $\mu$ L/tube of 1,1,1,3,3,3-hexafluoro-2-propanol (HFIP) (Kanto Chemical Co.,Inc.) was added to A $\beta$  after drying in a centrifugal evaporator, and the solution was re-dissolved. The cells were again dried in a centrifugal evaporator and stored at  $-20^{\circ}\text{C}$  until use. The day before cell addition, the dried A $\beta$  was dissolved in 40  $\mu$ L of dimethyl sulfoxide (DMSO) (Merck KGaA) (2.5 mg/mL) and further diluted 25-fold by adding 960  $\mu$ L of medium (final A $\beta$  concentration: 100  $\mu$ g/mL = 20  $\mu$ M, DMSO concentration: 4%). A $\beta$  diluted in medium was incubated at  $4^{\circ}\text{C}$  for 24 hours to oligomerize A $\beta$ .

#### **Experimental procedure: Verification of A $\beta$ phagocytosis**

BV2 cells, which had been cultured until sufficient volume was reached by passaging, were seeded in 96-well plates at a density of  $5 \times 10^3$  cells/well. The day after seeding, supplemental medium was prepared at the following concentrations and added at 100  $\mu$ L/well.

Negative control	A $\beta$ : None	DMSO: 0.2%	
Positive control	A $\beta$ : 1 $\mu$ M	DMSO: 0.2%	
Yeast EV			
× 100	A $\beta$ : 1 $\mu$ M	DMSO: 0.2%	EV: 1%
× 1,000	A $\beta$ : 1 $\mu$ M	DMSO: 0.2%	EV: 0.1%
× 10,000	A $\beta$ : 1 $\mu$ M	DMSO: 0.2%	EV: 0.01%
SCST-A			
× 2	A $\beta$ : 1 $\mu$ M	DMSO: 0.2%	HGF: 50 ng/mL
× 20	A $\beta$ : 1 $\mu$ M	DMSO: 0.2%	HGF: 5 ng/mL
× 200	A $\beta$ : 1 $\mu$ M	DMSO: 0.2%	HGF: 0.5 ng/mL
SCST-B			
× 2	A $\beta$ : 1 $\mu$ M	DMSO: 0.2%	HGF: 5 ng/mL
× 5	A $\beta$ : 1 $\mu$ M	DMSO: 0.2%	HGF: 2 ng/mL
× 20	A $\beta$ : 1 $\mu$ M	DMSO: 0.2%	HGF: 0.5 ng/mL

(Note that HGF is an estimated concentration)

At 24 hours after addition, the supernatant was removed, washed once with HBSS (-), and 100  $\mu$ L of phenol red-free medium was added. The cells were then observed with an all-in-one microscope (BZX-710, Keyence). From the TAMRA-A $\beta$  fluorescence and phase contrast images, image analysis was performed to calculate the TAMRA fluorescence intensity per image and the total area value of cells.

Formula:

TAMRA fluorescence intensity / total area value of cells

The TAMRA fluorescence intensity was corrected for the total area value of the cells, and the control ratio of each group to the negative control group (% NC) and the control ratio of each group to the A $\beta$ -supplemented group (positive control) (% A $\beta$ ) were calculated and graphed.

### Stem cell-derived secretome (SCST)

Two types of cell supernatants were used in this study. The first was the same SCST used in the previous report<sup>4)</sup>, and freeze-dried mesenchymal SCST (SCST-A) was used (Nature Bionics, Inc., Tokyo). When dissolved in 1 mL, one vial contains approximately  $1 \times 10^8$  exosomes and  $1.2 \times 10^5$  pg/mL of hepatocellular growth factor (HGF), one of the main growth factors, as well as many other types of growth factors, nutritional factors, cytokines, etc. In addition to HGF, the product is manufactured to meet the respective index amounts for several representative components, so that the active ingredients are almost the same in amount and there is little difference between lots.

The donors of the stem cells were healthy Japanese women in their 20s and 30s, and a completely serum-free medium was used without insulin or antibiotics and without animal or human serum to avoid the risk of viral infection. Unnecessary components such as ammonia, which are produced in large quantities during the cultivation process, are removed to below the detection limit, and active components such as various growth factors and exosomes are concentrated.

The second SCST sample (SCST B) was provided by a medical institution in Japan. They say it contains an estimated HGF concentration of 5 ng/mL. It also contains exosomes and growth factors, but the amount contained is unknown.

Yeast-derived extracellular vesicles (EV) were used for comparison. Yeast-derived EV (Yeast EV) used was YSEV-R3 (Cosmo Bio).

### Verification of gene expression: Microarray method

BV2 cells were passaged to reach sufficient volume and seeded into 100-mm dishes at a density of about  $1.6 \times 10^6$  cells per dish. The day after seeding, medium for addition was prepared to the following concentrations of A $\beta$  and DMSO and added at 10 mL/dish by changing the medium. 24 hours after addition, the supernatant was removed, the cells were lysed, and total RNA was extracted. After extraction, microarray analysis was performed by MacroGen Japan (Tokyo).

Negative control	A $\beta$ : None	DMSO: 0.3%
Positive control	A $\beta$ : 1 $\mu$ M	DMSO: 0.3%

## Results

### Microglia A $\beta$ phagocytosis

**Figures 1** and **2** show the culture status of microglia-derived BV2 cells as fluorescence and phase contrast microscopic images.

TAMRA fluorescence was not detectable in the A $\beta$  non-added group (negative control), whereas fluorescence was detectable in the A $\beta$  added group (positive control). It was difficult to evaluate by image observation alone whether the addition of yeast EV or SCST changed the microglia A $\beta$  phagocytosis.

In **Tables 1** and **2**, the fluorescence intensity of each was measured and used as an index of microglia A $\beta$  phagocytosis. Each group consisted of  $n = 4$ . Since differences in measurement conditions caused differences in the measured values of the positive control, negative and positive controls were established for each plate.

**Figure 3** shows the ratio of fluorescence intensity to the positive control. Only the mesenchymal SCST-A used in the previous clinical study<sup>4)</sup> enhanced microglia A $\beta$  phagocytosis in a dose-dependent manner.

### Microarray analysis

To verify whether A $\beta$  is actually taken up by microglia and exerts its effects at the molecular level, we analyzed the changes in gene expression using microarrays. The results of the Gene Ontology (GO) analysis are classified into three categories: biological process (**Fig. 4-a**), cellular component (**Fig. 4-b**), and molecular function (**Fig. 4-c**). In the biological process, gene expression changes were observed in the regulation of cellular processes, regulation of biological processes, biological regulation, cellular response to stimuli, and signal transduction. In the cellular component, gene expression changes were observed in the anatomical entity of cells. In the molecular function, gene expression changes were observed in signal receptor activity, signal transduction system, transmembrane receptor activity, and G protein-coupled receptor activity.

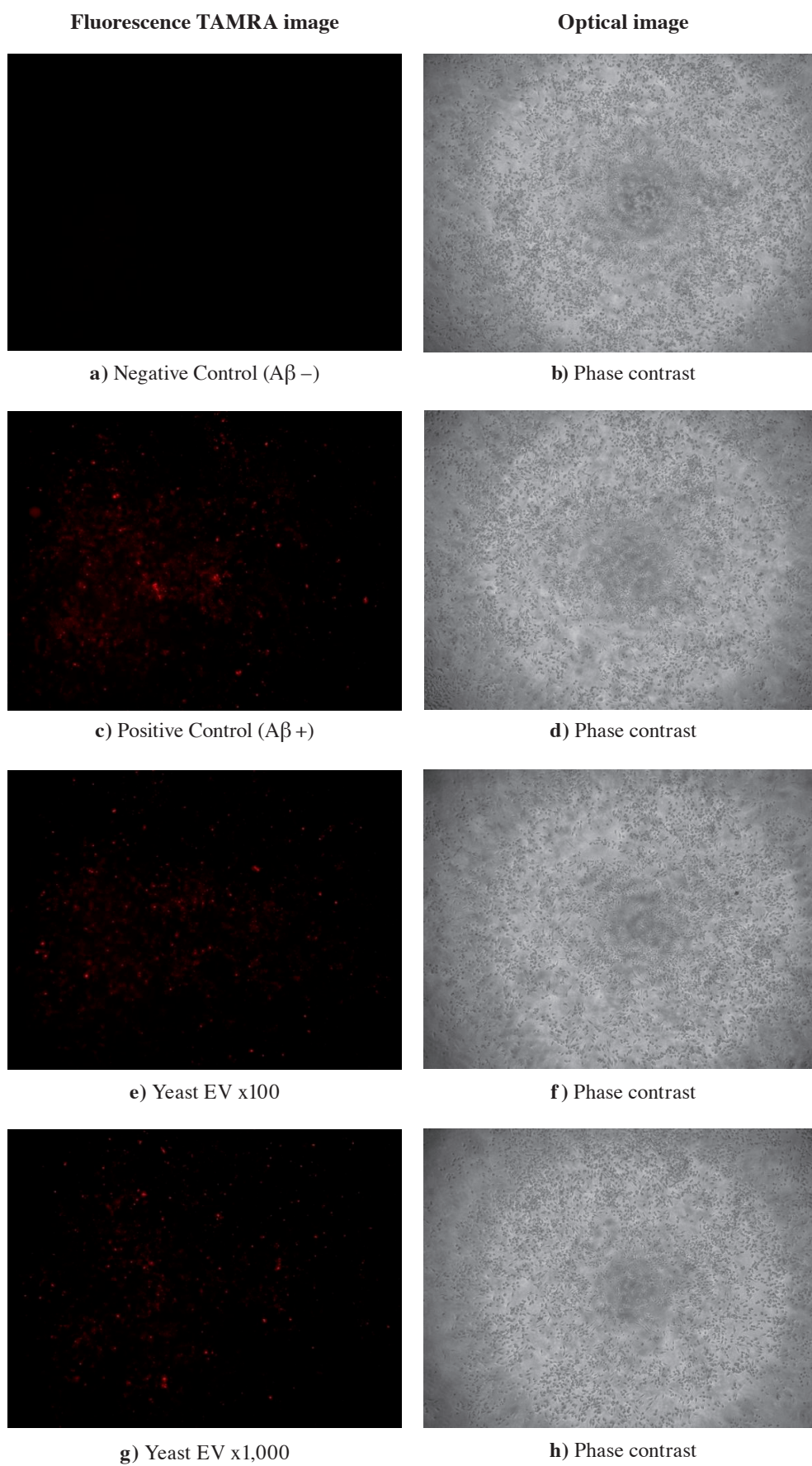


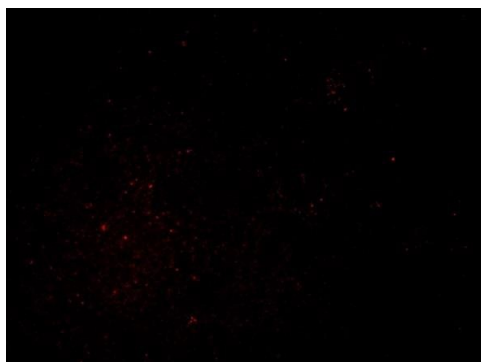
**Fig.1. Cultured microglia image (Plate 1).**

EV, extracellular vesicle.

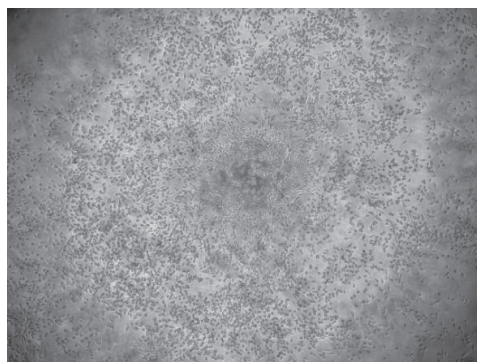


**Fluorescence TAMRA image**

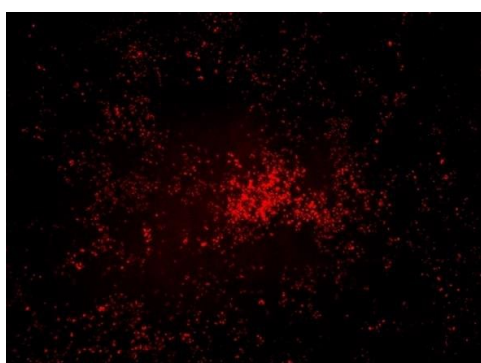
**Optical image**



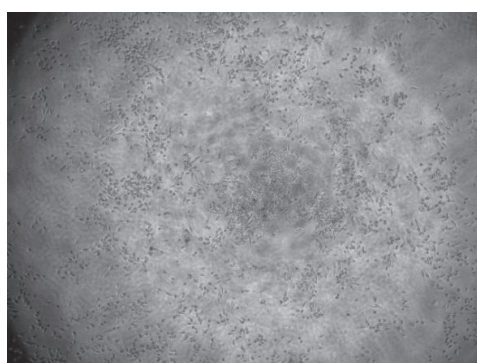
**a) Yeast EV x10,000**



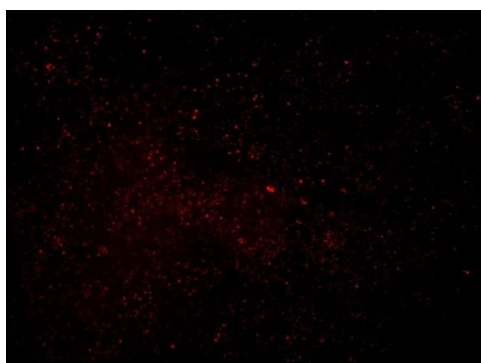
**b) Phase contrast**



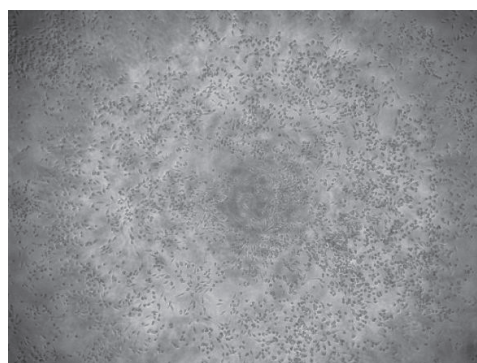
**c) SCST-A x2**



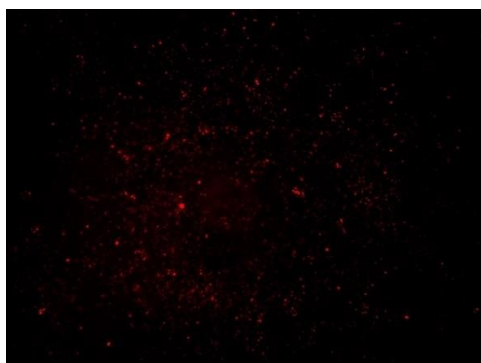
**d) Phase contrast**



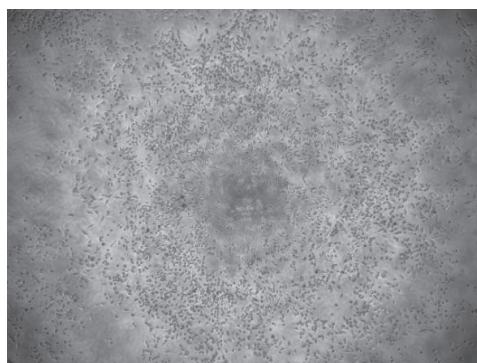
**e) SCST-A x20**



**f) Phase contrast**



**j) SCST-A x200**



**h) Phase contrast**

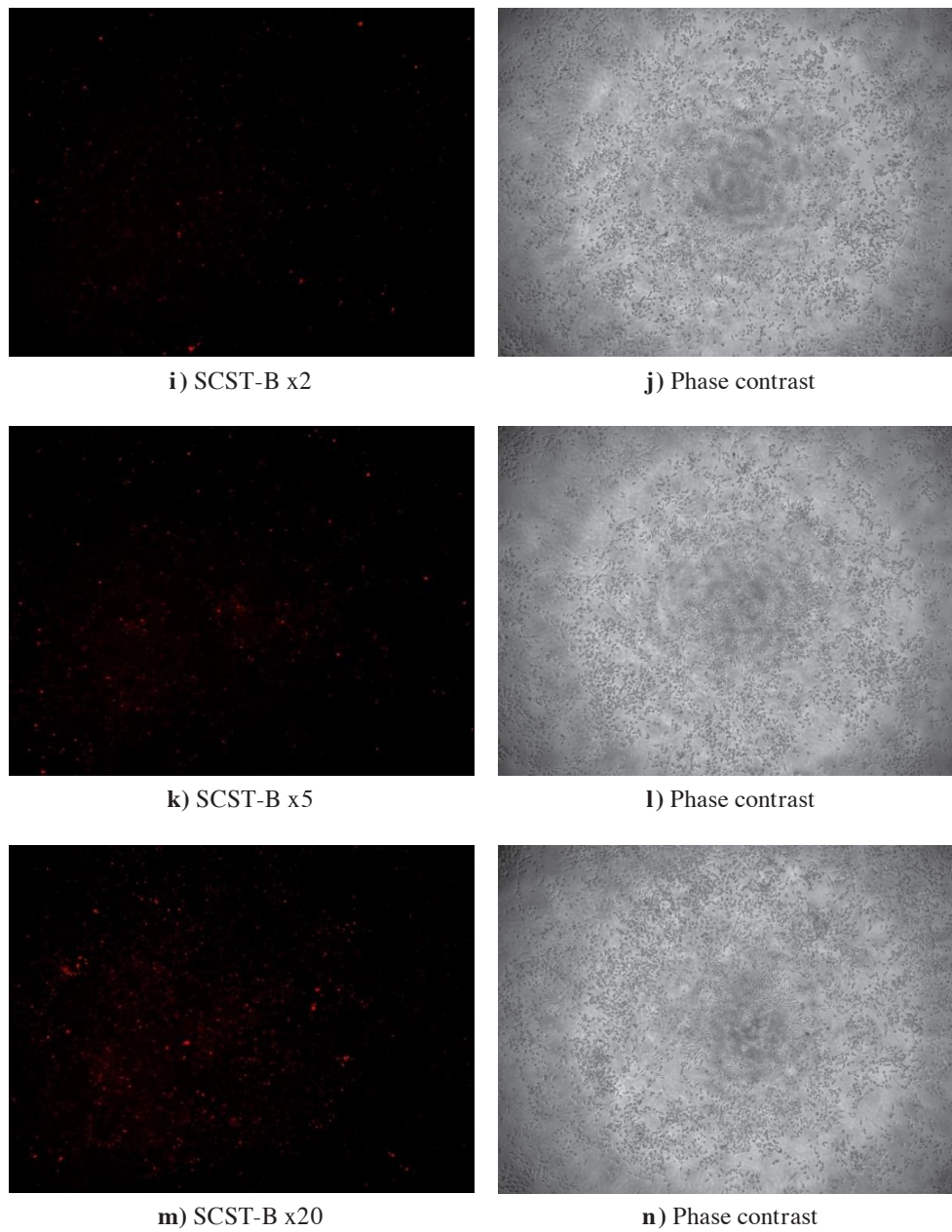


**Fig.2. Cultured microglia image (Plate 2).**

EV, extracellular vesicle. SCST, mesenchymal stem cell-derived secretome.

**Table 1. Results of fluorescence intensity: A $\beta$  phagocytosis index (Plate 1).**

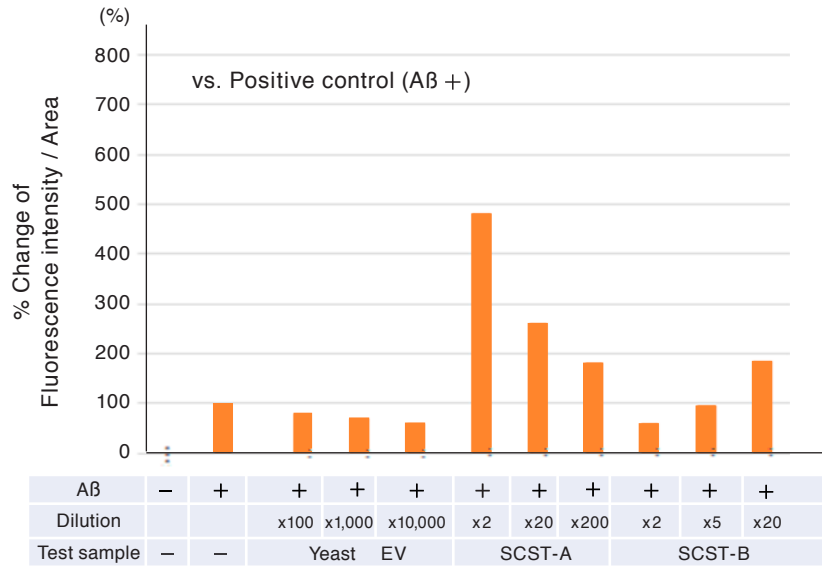
Group (Plate 1)	FI (Integrated)	Area (Integrated)	FI/Area (Corrected)	Average	SEM	% NC	% PC
Negative control (NC) A $\beta$ (-)	5,662	5,886,304	9.62.E-04	2.57.E-04	2.03.E-04	100%	-
	108	5,173,551	2.09.E-05				
	135	6,504,722	2.08.E-05				
	162	6,253,515	2.59.E-05				
Positive control (PC) A $\beta$ (+)	604,653	4,816,245	1.26.E-01	1.51.E-01	1.33.E-02	58,529%	100%
	720,560	5,875,886	1.23.E-01				
	1,163,465	6,7042,90	1.74.E-01				
	1,332,503	7,369,924	1.81.E-01				
	978,860	6,210,947	1.58.E-01				
	756,885	6,543,283	1.16.E-01				
	871,041	6,453,243	1.35.E-01				
Yeast EV x100 A $\beta$ (+)	395,331	4,434,738	8.91.E-02	1.20.E-01	1.03.E-02	46,600%	80%
	746,704	6,398,303	1.17.E-01				
	820,308	6,409,137	1.28.E-01				
	915,831	6,278,260	1.46.E-01				
Yeast EV x1,000 A $\beta$ (+)	295,519	4,741,174	6.23.E-02	1.03.E-01	1.37.E-02	39,831%	68%
	471,174	3,434,813	1.37.E-01				
	494,521	4,304,150	1.15.E-01				
	422,725	4,420,153	9.56.E-02				

FI, fluorescence intensity; SEM, standard error mean; EV, extracellular vesicle.

**Table 2. Results of fluorescence intensity: A $\beta$  phagocytosis index (Plate 2).**

Group (Plate 2)	FI (Integrated)	Area (Integrated)	FI/Area (Corrected)	Average	SEM	% NC	% PC
Negative control A $\beta$ (-)	5	5,825,113	8.58.E-07	2.20.E-04	1.83.E-04	100%	-
	28	7,062,462	3.96.E-06				
	132	6,300,474	2.10.E-05				
	5,839	6,845,136	8.53.E-04				
Positive control A $\beta$ (+)	264,613	6,015,738	4.40.E-02	6.00.E-02	1.01.E-02	27,333%	100%
	264,740	5,136,753	5.15.E-02				
	259,160	5,192,431	4.99.E-02				
	554,611	5,852,807	9.48.E-02				
Yeast EV x10,000 A $\beta$ (+)	163,736	6,176,329	2.65.E-02	3.56.E-02	4.21.E-03	16,198%	59%
	196,163	5,547,236	3.54.E-02				
	168,509	5,372,446	3.14.E-02				
	321,880	6,555,047	4.91.E-02				
	1,103,828	5,097,519	2.17.E-01				
	875,578	4,886,988	1.79.E-01				
	1,525,473	5,143,644	2.97.E-01				
SCST-A x2 A $\beta$ (+)	1,277,428	2,781,199	4.59.E-01	2.89.E-01	5.04.E-02	131,519%	481%
	1,054,059	4,444,514	2.37.E-01				
	913,478	4,601,226	1.99.E-01				
	1,285,373	4,929,043	2.61.E-01				
SCST-A x20 A $\beta$ (+)	647,831	4,160,483	1.56.E-01	1.56.E-01	3.61.E-03	70,917%	259%
	854,001	5,840,659	1.46.E-01				
	974,431	5,850,179	1.67.E-01				
	895,619	5,788,828	1.55.E-01				
SCST-A x200 A $\beta$ (+)	491,261	4,412,781	1.11.E-01	1.09.E-01	1.66.E-03	49,771%	182%
	620,828	5,920,794	1.05.E-01				
	696,461	6,465,712	1.08.E-01				
	721,674	6,359,165	1.13.E-01				
SCST-B x2 A $\beta$ (+)	137,547	4,530,323	3.04.E-02	3.55.E-02	5.40.E-03	16,178%	59%
	164,859	5,775,365	2.85.E-02				
	161,843	5,569,193	2.91.E-02				
	281,414	5,191,789	5.42.E-02				
SCST-B x5 A $\beta$ (+)	262,819	4,586,097	5.73.E-02	5.76.E-02	1.27.E-03	26,215%	96%
	332,899	6,202,677	5.37.E-02				
	371,320	6,127,799	6.06.E-02				
	381,500	6,488,118	5.88.E-02				
SCST-B x20 A $\beta$ (+)	448,949	5,450,273	8.24.E-02	1.10.E-01	1.40.E-02	50,232%	184%
	327,562	3,844,944	8.52.E-02				
	565,440	3,778,175	1.50.E-01				
	417,598	3,362,082	1.24.E-01				

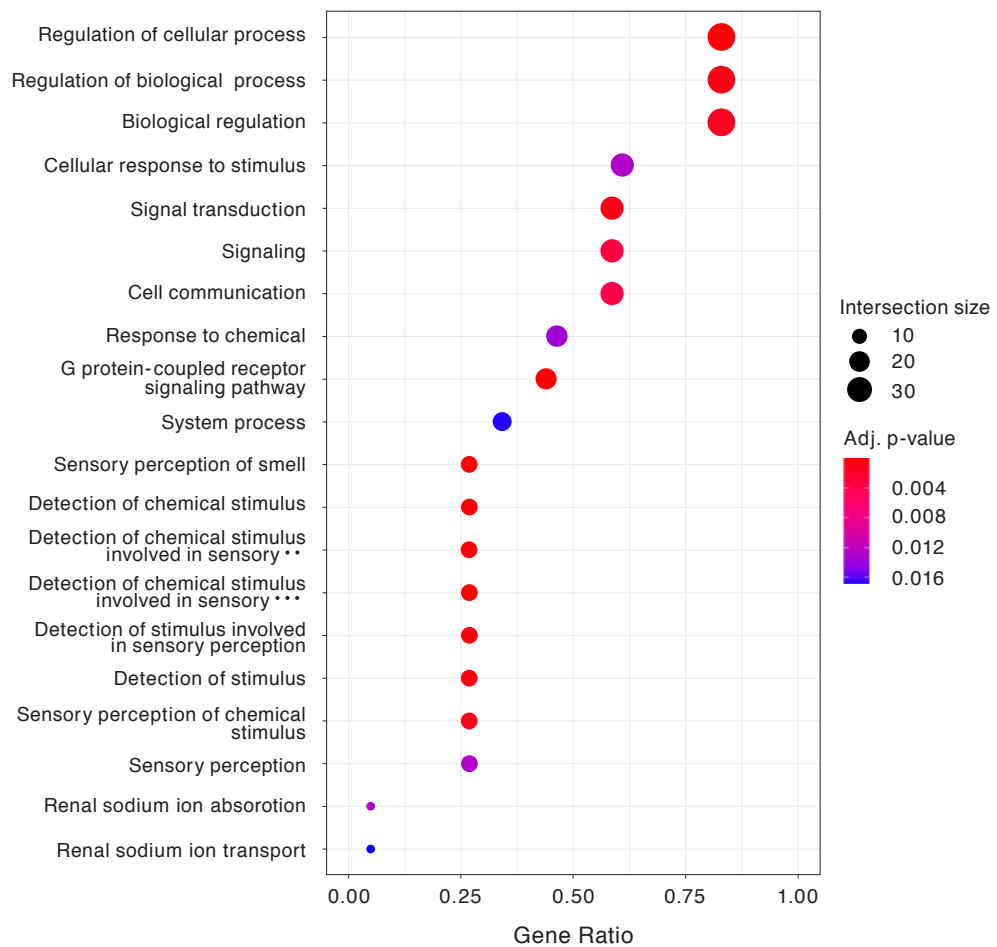
FI, fluorescence intensity; SEM, standard error mean; EV, extracellular vesicle; SCST, mesenchymal stem cell-derived secretome.



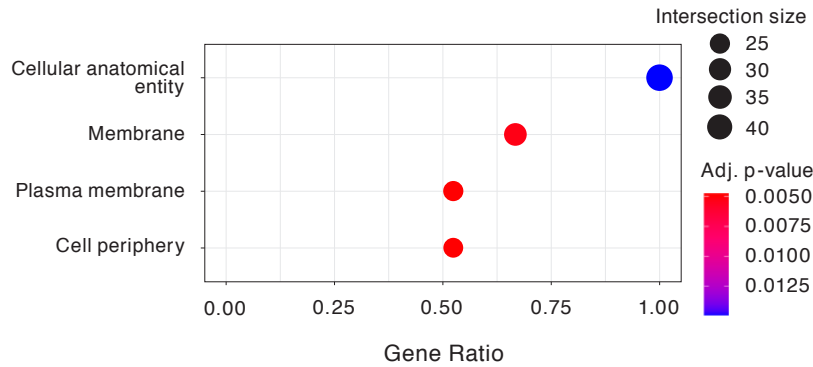
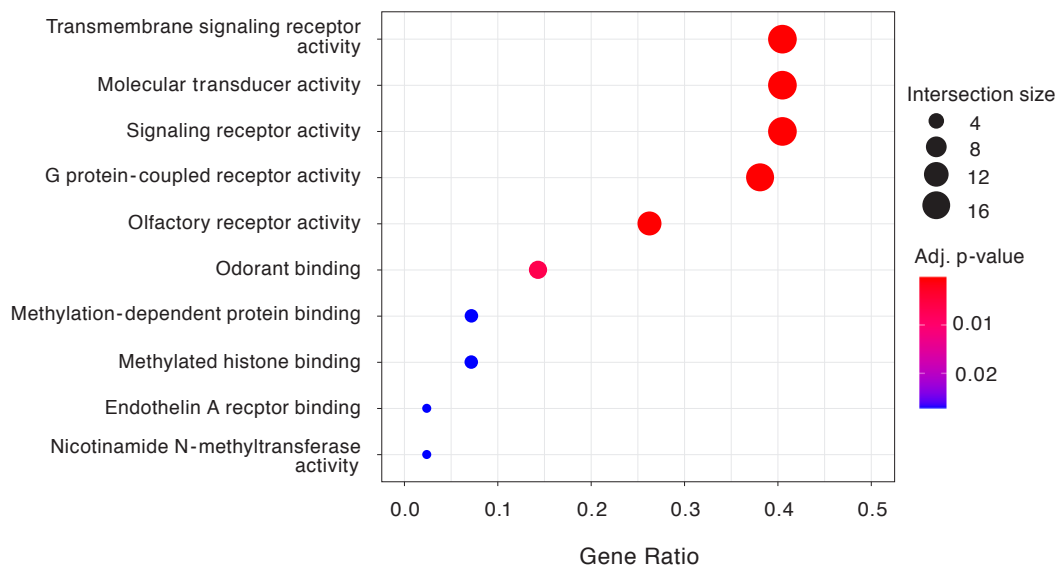
**Fig. 3. Microglia Aβ phagocytosis potential: Comparison with positive control.**

Results are expressed as % change of fluorescence intensity derived from TMRA-Aβ uptaken by microglia VB2 cell (data from Table 1 & 2). EV, extracellular vesicle; SCST, mesenchymal stem cell-derived secretome.

**Fig. 4-a.**





**Fig. 4-b.****Fig. 4-c.****Fig. 4. Microarray GO functional analysis.**

**a)** Biological process. **b)** Cellular component. **c)** Molecular function.

Results are expressed as Gene Ratio (intersection-size/query-size). GO, gene ontology.

## Discussion

Glial cells (astrocytes, oligodendrocytes, and microglia) play important roles in supporting the activity of the central nervous system (CNS), maintaining the tissue environment, providing nutrition, and clearing  $A\beta$ . Damage to glial cells also has a negative effect on the CNS<sup>12</sup>. Factors that cause damage to glial cells include inflammation, oxidative stress (OS), and GS<sup>13</sup>. Although the term “metabolic stress” has often been used, in this paper we refer to it as GS, as excess aldehydes are involved in most cases. Reducing these factors and aiming for glioprotection is extremely important for maintaining homeostasis of the CNS.

Many  $A\beta$  removal therapies have been attempted to date, however, there have been many adverse events and no successful cases. The current situation is that therapeutic drugs are being developed with the main pharmacological effects being the inhibition of  $A\beta$  production mechanism

by controlling secretase activity, the inhibition of amyloid formation by inhibiting  $A\beta$  aggregation, and the inhibition of amyloid deposition to promote  $A\beta$  removal. It has been shown that the  $A\beta$  clearance rate is significantly decreased in patients with sporadic AD<sup>14</sup>, and the complete picture of the metabolic pathway of  $A\beta$  degradation is awaited.

According to Dahlgren KN et al., early in vitro studies suggested that  $A\beta$ -induced neurotoxicity required the peptide to adopt a fibrillar aggregated state, and that low doses of non-aggregated peptides were indeed neurotrophic<sup>2</sup>. Their validation showed that oligomeric  $A\beta$ -(1-42) significantly reduced neuronal viability, whereas non-aggregated peptides had less effect on viability. Non-aggregated  $A\beta$  showed a biphasic response, exerting neurotrophic effects at low concentrations (1–100  $\mu$ M) and neurotoxicity at higher concentrations (1–15  $\mu$ M). Non-aggregated  $A\beta$ -(1-40) had no significant effect on neuronal viability even at 20  $\mu$ M, and at concentrations below 1  $\mu$ M appeared to be as neurotrophic as

non-aggregated A $\beta$ -(1-42) preparations. Supporting the CNS by maintaining the health of microglia's A $\beta$  phagocytosis, restoring its reduced function, and promoting its activity may also be effective in preventing the progression of dementia (especially AD), and new treatment strategies are expected.<sup>15-21</sup> Metformin<sup>16,22</sup>, curcumin<sup>23,24</sup>, and resveratrol<sup>23,25</sup> not only have anti-oxidation functions, but also have anti-glycation effects that inhibit the formation of advanced glycation products (AGEs). These findings suggest that GS care is important in gliaprotection as well.

On the other hand, oxidation and lipid loading induce a decline in microglia function<sup>26</sup>. Restoration of mitochondrial function also restores A $\beta$  phagocytosis<sup>27</sup>. Oxidation and lipid loading induce the oxidation of FAs, enhancing the formation of FA-derived aldehydes, leading to an excess state. Glyceraldehyde-3-phosphate dehydrogenase (GAPDH) and aldehyde dehydrogenase (ALDH) consume NAD (nicotinamide adenine dinucleotide) in the process of metabolizing aldehydes, and NAD is also consumed in the process of  $\beta$ -oxidation enhanced by lipid loading. As a result, NAD becomes insufficient in the TCA cycle in mitochondria, subsequently ATP production decreases, and ultimately the cellular function of microglia is weakened.

Deposition of aldehyde-modified proteins such as MGO and Acro has been observed in senile plaques (amyloid plaques) by immunohistochemistry<sup>28-38</sup>, the presence of glycated A $\beta$  is strongly suspected. It has been pointed out that urinary aldehyde-modified proteins may be an indicator of dementia<sup>39</sup>.

In the lipid-rich brain, important proteins are vulnerable to a double whammy attack from not only carbohydrate-derived aldehydes (*i.e.*, GO [glyoxal], MGO, 3DG [3-deoxyglucosone], GA [glyceraldehyde]) but also FA-derived aldehydes (*i.e.*, MGO, Acro, MDA [malondialdehyde], etc.)<sup>40-42</sup> produced by the oxidation of FAs<sup>13</sup>.

In our previous study, we reported that MGO and Acro-modified A $\beta$  are difficult to phagocytose by microglia<sup>1</sup>. This result suggests that aldehyde modification of A $\beta$  due to GS may be the cause of reduced A $\beta$  clearance. In the subsequent clinical study<sup>4</sup>, we reported that nasal administration of SCST may lead to improvement of symptoms in dementia patients. In order to explore the mechanism of improvement, this study examined the effect on microglia A $\beta$  phagocytosis, which is one of the indicators of A $\beta$  clearance.

The SCST contains various growth factors and EVs. Among them, HGF is a physiologically active protein that is responsible for regeneration of the liver and kidney and protection of neural tissue. It is known as the most powerful growth factor for hepatocytes and is also produced in organs other than the liver<sup>43</sup>. HGF strongly promotes the proliferation of primary cultured mature rat hepatocytes at concentrations of 1 ng/mL or more<sup>44</sup>. The HGF concentration in human serum is high in patients with fulminant hepatitis, averaging approximately 10 ng/mL. In patients with acute hepatitis, liver cirrhosis, and liver cancer, the levels are 2-3 times higher than in healthy adults (approximately 0.2 ng/mL), but rarely exceed 1 ng/mL. The estimated HGF concentration in the culture medium of SCST-A $\times$ 200 (HGF: 0.5 ng/mL) is 2 to 3 times that of healthy adults. The results of this experiment showed that the SCST administration increases microglia A $\beta$  phagocytosis in a dose-dependent manner. Nasal SCST administration may have a similar effect and contribute to

improving A $\beta$  clearance or maintaining homeostasis.

Of course, it is expected that the growth factors contained in SCST contribute to the protection and activation of neurons and glial cells. Since neurons in the hippocampal dentate gyrus, which are deeply involved in memory function, maintain their division and proliferation functions even in the elderly, it is expected that activation of these cell functions will greatly contribute to the improvement of dementia symptoms. This test did not clarify to what extent the active ingredient is transferred into the brain parenchyma by nasal administration, that can be a future topic of research.

### *Molecular impacts of A $\beta$ on microglia*

To verify whether A $\beta$  is actually taken up by microglia and has an impact at the molecular level, we analyzed the changes in gene expression using microarrays. Genes with significant changes in expression were extracted in the categories of biological process, cellular component, and molecular function. It was shown that the A $\beta$  administration had an impact on microglia gene expression. In this analysis, A $\beta$  oligomers were used, and different results may be obtained with non-aggregated A $\beta$ . Later, we plan to analyze the changes in the expression state of individual genes over time to see whether A $\beta$  is involved in gliaprotection. It is an extremely interesting question which genes are affected by SCST.

### *Microglia A $\beta$ phagocytosis model*

In this study, we have established an evaluation model for microglia A $\beta$  phagocytosis. We placed emphasis on reproducibility so that the efficacy of various test substances can be compared and evaluated also at other facilities.

When preparing the model, we considered whether to use primary cultured cells or lineage cultured cell lines as microglia. The former is assumed to retain the characteristics of microglia at a high level, but they need to be collected from animals for each experiment, and there is a possibility of individual differences and differences due to techniques. The latter may have lost some of the microglia characteristics, but it expectedly has higher reproducibility. The latter was selected as a model that requires multiple experiments over a long period of time and analyzes multiple comparative factors.

We selected the A $\beta$  to be used. This was because TAMRA-A $\beta$ , which was used in the previous report<sup>1</sup>, was discontinued. We examined the addition of fluorescent labels, changes in properties due to aldehyde modification and the creation of oligo- and fibril bodies, and the compatibility and cytotoxicity between primary cultured microglia and culture strains. As a result, we used newly synthesized A $\beta$ . The details of this research will be reported separately.

Next, Polaric (Cosmo Bio) and TAMRA were compared as fluorescent dyes for labeling A $\beta$ . After fluorescent labeling of A $\beta$ , oligomeric and fibril bodies were prepared as previously reported<sup>2</sup> and the fluorescence intensity was evaluated. TAMRA-A $\beta$  was selected, which showed little change in fluorescence intensity after phagocytosis.

Regarding measurement methods, a method using a confocal laser microscope and an all-in-one fluorescence microscope were compared. The former is suitable for taking beautiful photographs, but requires separate image analysis using a separate device, making the process complicated.

With the latter, the process of taking photographs under fixed conditions, saving the photo files, and analyzing the images can all be done with a single device, and the procedure is less complicated than the former. This is the reason for selecting the latter for the model.

## Conclusion

We evaluated microglia A $\beta$  phagocytosis using SCST, which was reported to improve the symptoms of dementia patients in a previous study<sup>4)</sup>. The results showed that the SCST addition may increase phagocytosis activity in a dose-dependent manner. Microarray analysis showed that various gene expressions were induced during A $\beta$  phagocytosis. In the future, we plan to verify whether the SCST addition to microglia is effective for gliaprotection and analyze what changes occur in gene expression.

## Research grants

This research was supported by a Grant-in-Aid for Scientific Research from the Ministry of Education, Culture, Sports, Science and Technology (KAKEN 23K10882).

## Conflict of Interest Declaration

None in particular.

## Reference

- 1) Yonei Y, Taira T, Otaka S, et al. Amyloid  $\beta$  clearance and microglia: Effects of glycativ stress and melatonin. *Glycative Stress Res.* 2022; 9: 135-145.
- 2) Dahlgren KN, Manelli AM, Stine WB Jr, et al. Oligomeric and fibrillar species of amyloid- $\beta$  peptides differentially affect neuronal viability. *J Biol Chem.* 2002; 277: 32046-32053.
- 3) Yonei Y. Factors influencing microglia A $\beta$  phagocytosis: Involvement of AGE degradation promoters and bacteria-derived EV. Issue #23K10882. 2023, April 13. (in Japanese) <https://kaken.nii.ac.jp/grant/KAKENHI-PROJECT-23K10882/>
- 4) Morita Y, Izawa H, Ohga H, et al. Safety and clinical efficacy on intranasal administration of mesenchymal stem cell-derived secretome in patients with Alzheimer's disease and its future prospect. *Glycative Stress Res.* 2024; 11: 103-110.
- 5) Xie X, Song Q, Dai C, et al. Clinical safety and efficacy of allogenic human adipose mesenchymal stromal cells-derived exosomes in patients with mild to moderate Alzheimer's disease: A phase I/II clinical trial. *Gen Psychiatr.* 2023; 36(5): e101143.
- 6) Lofty A, AboQuella NM, Wang H. Mesenchymal stromal/stem cell (MSC)-derived exosomes in clinical trials. *Stem Cell Res Ther.* 2023; 14: 66-83.
- 7) Goo J, Lee Y, Lee J, et al. Extracellular vesicles in therapeutics: A comprehensive review on applications, challenges, and clinical progress. *Pharmaceutics.* 2024; 16(3): 311.
- 8) Takenouchi T, Iwamaru Y, Sugama S, et al. The activation of P2X7 receptor induces cathepsin D-dependent production of a 20-kDa form of IL-1 $\beta$  under acidic extracellular pH in LPS-primed microglial cells. *J Neurochem.* 2011; 117: 712-723.
- 9) Cosmo Bio Co. Ltd. Primary Microglia Culture Kit (SD rat), Code No. MGSD. Attachment. [https://search.cosmobio.co.jp/cosmo\\_search\\_p/search\\_gate2/docs/PMC\\_/MGSD.20181218.pdf](https://search.cosmobio.co.jp/cosmo_search_p/search_gate2/docs/PMC_/MGSD.20181218.pdf) Accessed at November 30, 2024. (in Japanese)
- 10) Sama P, Long TC, Hester S, et al. The cellular and genomic response of an immortalized microglia cell line (BV2) to concentrated ambient particulate matter. *Inhal Toxicol.* 2007; 19: 1079-1087.
- 11) Moniruzzaman M, Lee G, Bose S, et al. Antioxidant and anti-inflammatory activities of N-((3,4-dihydro-2H-benzo[h]chromene-2-yl)methyl)-4-methoxyaniline in LPS-induced BV2 microglial cells. *Biol Pharm Bull.* 2015; 38: 1831-1835.
- 12) Quincozes-Santos A, Santos CL, de Souza Almeida RR, et al. Gliotoxicity and glioprotection: The dual role of glial cells. *Mol Neurobiol.* 2021; 58: 6577-6592.
- 13) Yonei Y, Yagi M, Sato K, et al. Glycative stress: Molecular impacts and defense mechanisms. *Glycative Stress Res.* 2023; 10: 145-158.
- 14) Mawuenyega KG, Sigurdson W, Ovod V, et al. Decreased clearance of CNS  $\beta$ -amyloid in Alzheimer's disease. *Science.* 2010; 330(6012): 1774.
- 15) Kim H, Le B, Goshi N, et al. Primary cortical cell triculture to study effects of amyloid- $\beta$  on microglia function and neuroinflammatory response. *J Alzheimers Dis.* 2024; 13872877241291142.
- 16) Guo X, Zhang B, Chen Y, et al. Multifunctional mesoporous nanoselenium delivery of metformin breaks the vicious cycle of neuroinflammation and ROS, promotes microglia regulation and alleviates Alzheimer's disease. *Colloids Surf B Biointerfaces.* 2024; 245: 114300. doi: 10.1016/j.colsurfb.2024.114300.
- 17) Feng Q, Zhang X, Zhao X, et al. Intranasal delivery of pure nanodrug loaded liposomes for Alzheimer's disease treatment by efficiently regulating microglial polarization. *Small.* 2024; e2405781.
- 18) Jiang M, Zhao D, Zhou Y, et al. Cathepsin B modulates microglial migration and phagocytosis of amyloid  $\beta$  in Alzheimer's disease through PI3K-Akt signaling. *Neuropsychopharmacology.* 2024 Sep 20.
- 19) Aerbajinai W, Zhu J, Chin K, et al. Glia maturation factor-gamma regulates amyloid- $\beta$ 42 phagocytosis through scavenger receptor AI in murine macrophages. *J Leukoc Biol.* 2024; qiae197. doi: 10.1093/jleuko/qiae197.

- 20) Piccioni G, Maisto N, d'Ettoire A, et al. Switch to phagocytic microglia by CSFR1 inhibition drives amyloid- $\beta$  clearance from glutamatergic terminals rescuing LTP in acute hippocampal slices. *Transl Psychiatry*. 2024; 14: 338.
- 21) Aljohani NB, Qusti SY, Alsiny M, et al. Carboxymethylcellulose encapsulated fingolimod, siRNA @ZnO hybrid nanocomposite as a new anti-Alzheimer's material. *RSC Adv*. 2024; 14: 22044-22055.
- 22) Kiho T, Kato M, Usui S, et al. Effect of buformin and metformin on formation of advanced glycation end products by methylglyoxal. *Clin Chim Acta*. 2005; 358: 139-145.
- 23) Banaszak M, Górna I, Woźniak D, et al. The impact of curcumin, resveratrol, and cinnamon on modulating oxidative stress and antioxidant activity in type 2 diabetes: Moving beyond an anti-hyperglycaemic evaluation. *Antioxidants (Basel)*. 2024; 13: 510.
- 24) Abbas W, Alam Khan R, Tasawar Baig M, et al. Effect of *Curcuma longa* on glycemia, neuropathic sensation and advanced glycation end product in diabetic patients. *Pak J Pharm Sci*. 2022; 35: 873-878.
- 25) Huang CY, Chen SH, Lin T, et al. Resveratrol attenuates advanced glycation end product-induced senescence and inflammation in human gingival fibroblasts. *J Dent Sci*. 2024; 19: 580-586.
- 26) Lin D, Gold A, Kaye S, et al. Arachidonic acid mobilization and peroxidation promote microglial dysfunction in A $\beta$  pathology. *J Neurosci*. 2024; 44: e0202242024.
- 27) Tang Y, Wang Y, Gao Z, et al. sAPP $\alpha$  peptide promotes damaged microglia to clear Alzheimer's amyloid- $\beta$  via restoring mitochondrial function. *Chemistry*. 2024; 30: e202400870.
- 28) Kuhla B, Lüth HJ, Haferburg D, et al. Methylglyoxal, glyoxal, and their detoxification in Alzheimer's disease. *Ann N Y Acad Sci*. 2005; 1043: 211-216.
- 29) Ahmed N, Ahmed U, Thornalley PJ, et al. Protein glycation, oxidation and nitration adduct residues and free adducts of cerebrospinal fluid in Alzheimer's disease and link to cognitive impairment. *J Neurochem*. 2005; 92: 255-263.
- 30) Beeri MS, Moshier E, Schmeidler J, et al. Serum concentration of an inflammatory glycotoxin, methylglyoxal, is associated with increased cognitive decline in elderly individuals. *Mech Ageing Dev*. 2011; 132: 583-587.
- 31) Angeloni C, Zamboni L, Hrelia S. Role of methylglyoxal in Alzheimer's disease. *Biomed Res Int*. 2014; 2014: 238485.
- 32) Dang TN, Arseneault M, Murthy V, et al. Potential role of acrolein in neurodegeneration and in Alzheimer's disease. *Curr Mol Pharmacol*. 2010; 3: 66-78.
- 33) Waragai M, Yoshida M, Mizoi M, et al. Increased protein-conjugated acrolein and amyloid- $\beta$  40/42 ratio in plasma of patients with mild cognitive impairment and Alzheimer's disease. *J Alzheimers Dis*. 2012; 32: 33-41.
- 34) Huang YJ, Jin MH, Pi RB, et al. Acrolein induces Alzheimer's disease-like pathologies *in vitro* and *in vivo*. *Toxicol Lett*. 2013; 217: 184-191.
- 35) Igarashi K, Yoshida M, Waragai M, et al. Evaluation of dementia by acrolein, amyloid- $\beta$  and creatinine. *Clin Chim Acta*. 2015; 450: 56-63.
- 36) Tsou HH, Hsu WC, Fuh JL, et al. Alterations in acrolein metabolism contribute to Alzheimer's disease. *J Alzheimers Dis*. 2018; 61: 571-580.
- 37) Chen C, Chen Y, Lu J, et al. Acrolein-conjugated proteomics in brains of adult C57BL/6 mice chronically exposed to acrolein and aged APP/PS1 transgenic AD mice. *Toxicol Lett*. 2021; 344: 11-17.
- 38) Chen C, Lu J, Peng W, et al. Acrolein, an endogenous aldehyde induces Alzheimer's disease-like pathologies in mice: A new sporadic AD animal model. *Pharmacol Res*. 2022; 175: 106003.
- 39) Yoshida M, Uemura T, Mizoi M, et al. Urinary amino acid-conjugated acrolein and taurine as new biomarkers for detection of dementia. *J Alzheimers Dis*. 2023; 92: 361-369.
- 40) Araujo LCC, Bordin S, Carvalho CRO. Reference gene and protein expression levels in two different NAFLD mouse models. *Gastroenterol Res Pract*. 2020; 2020: 1093235.
- 41) Fan X, Yao, H, Liu X, et al. High-fat diet alters the expression of reference genes in male mice. *Front Nutr*. 2020; 7: 589771.
- 42) Sato K, Zheng Y, Martin-Morales A, et al. Generation of short chain aldehydes and glyceraldehyde 3-phosphate dehydrogenase (GAPDH). *Glycative Stress Res*. 2022; 9: 129-134.
- 43) Gohda E. Function and regulation of production of hepatocyte growth factor (HGF). *Folia Pharmacol Jpn*. 2002; 119: 287-294. (in Japanese)
- 44) Gohda E, Tsubouchi H, Nakayama H, et al. Purification and partial characterization of hepatocyte growth factor from plasma of a patient with fulminant hepatic failure. *J Clin Invest*. 1988; 81: 414-419.